Title?

Jonathan R. J. Yong,[1] Ēriks Kupče,[2] Tim D. W. Claridge[1,*]

(What affiliations do we use?!)

[1] *Chemistry Research Laboratory, Department of Chemistry, University of Oxford, Mansfield Road, Oxford OX1 3TA, United Kingdom*

[2] *Bruker UK Ltd, R&D, Coventry CV4 9GH, United Kingdom*

[*] `tim.claridge@chem.ox.ac.uk`

Abstract

TOC PIC GOES HERE

- Detailed discussion of HSQC-COSY implementations in NMR supersequences.

- Comparison of HSQC-COSY with HSQC-TOCSY.

- Sensitivity analyses of modules within typical NMR supersequences involving HSQC-COSY experiments.

NMR supersequences, as exemplified by the NOAH (NMR by Ordered Acquisition using ^{1}Hdetection) technique, are a powerful way of acquiring multiple 2D data sets in much shorter durations. This is accomplished through targeted excitation and detection of the magnetisation belonging to specific isotopologues ('magnetisation pools'). Separately, the HSQC-COSY experiment has recently seen an increase in popularity due to the high signal dispersion in the indirect dimension and the removal of ambiguity traditionally associated with HSQC-TOCSY experiments. Here, we describe how the HSQC-COSY experiment can be integrated as a 'module' within NOAH supersequences. The benefits and drawbacks of several different pulse sequence implementations are discussed, with a particular focus on how sensitivities of other modules in the same supersequence are affected.

1 Introduction

The acceleration of multidimensional NMR spectroscopy has been an extremely popular topic in recent years, with techniques ranging from ultrafast NMR[1-3] and non-uniform sampling (NUS)[4-6] to multiple-receiver technology[7-9] and reduction of recovery delays.[10-12] NOAH (NMR by Ordered Acquisition using ^{1}H detection) experiments,[13] which fall under the category of multiple-FID experiments,[14] concatenate multiple 2D experiments ('modules') into a single nested pulse sequence with elision of intermediate recovery delays. Such 'supersequences' provide up to 4× time savings compared to conventional, one-by-one acquisition of each 2D spectrum, and have gained popularity due to their versatility as well as the fact that they do not require specialised hardware.
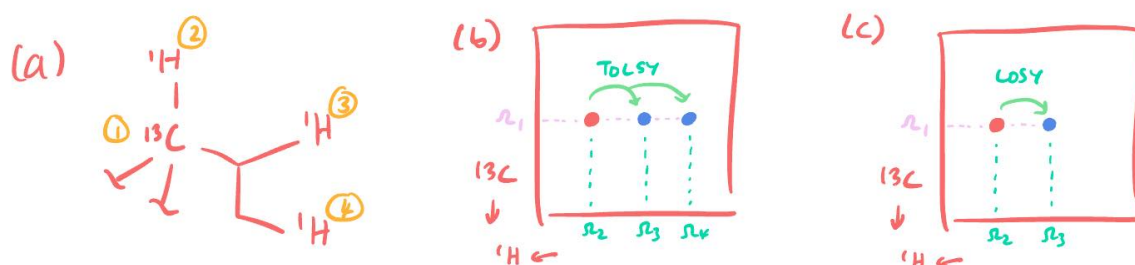

Figure 1: **(a)** A typical fragment of an organic molecule, with one ^{13}C and three ^{1}H spins. **(b)** The corresponding HSQC-TOCSY spectrum. The 'direct' peak at (Ω_1, Ω_2) is shown in red, and the 'indirect' peaks at (Ω_1, Ω_3) and (Ω_1, Ω_4) in blue: these have different signs due to an 'editing' spin echo described later in the text. **(b)** The corresponding HSQC-COSY spectrum, which is similar to the HSQC-TOCSY spectrum, except that there is only one 'indirect' peak which arises from coherence transfer over $^3J_{\text{HH}}$.

Virtually all of the most commonly used 2D experiments have been adapted for use within NOAH supersequences, as neatly listed on the GENESIS website.[15] In particular, we have previously described the implementation of the HSQC-TOCSY module in NOAH supersequences.[16] The HSQC-TOCSY experiment is extremely information-rich, providing both 'direct' responses which arise from directly bonded ^{13}C–^{1}H pairs, and 'indirect' responses from protons in the same spin system as those bound to ^{13}C (Figures 1a and 1b) This is essentially the same information as in separate HSQC and TOCSY spectra, but with the additional benefit that the TOCSY signals are dispersed more widely across the ^{13}C indirect dimension: this serves to greatly reduce the possibility of overlap and thus increase interpretability.

One downside of the HSQC-TOCSY is the largely indiscriminate transfer of magnetisation effected by the isotropic mixing block, which means that it is difficult to determine with certainty the number of bonds separating the ^{13}C and ^{1}H resonances in the 'indirect' responses. A direct method of overcoming this is to instead record an HSQC-COSY spectrum, where the 'indirect'

responses arise only from single-step coherence transfer between directly coupled ^{1}H–^{1}H pairs (Figure 1c). Experiments of this kind date back almost two decades, including the celebrated H2BC experiment,[17,18] and later 2BOB/H2OBC[19] and HMQC-COSY.[20] The 2BOB experiment in particular has previously been incorporated in NOAH supersequences.[21] Since then, the HSQC-CLIP-COSY[22,23] has emerged as a modern and improved experiment for this purpose: it provides pure absorption-mode lineshapes and does not suffer from amplitude modulation due to proton–proton couplings, a downside of the constant-time technique used in some of its predecessors.

Although the HSQC-CLIP-COSY performs admirably as a standalone experiment, the requirements for NOAH supersequences are more stringent: in particular, any HSQC-COSY module should—ideally—preserve unused magnetisation for later modules. The most important example of this is magnetisation of all protons not directly bound to ^{13}C (denoted[16,24] '^{1}H$^{!C}$'). The HSQC-COSY module does not use this 'magnetisation pool', and if it returns this magnetisation to the equilibrium $+z$ position, it can be sampled in a homonuclear module later in the supersequence. Another key feature of the NOAH HSQC-TOCSY module is the fact that it allows for variable excitation of ^{13}C–bound proton magnetisation (denoted '^{1}H^C'), meaning that a portion of it can be saved for a later heteronuclear module (e.g. an HSQC). We should therefore like any implementation of the HSQC-COSY to also exhibit this flexibility, as it allows the user to fine-tune the sensitivities of the modules within the supersequence for maximal performance.

In this work, we evaluate three different implementations of the NOAH HSQC-COSY module against several different criteria. These pulse sequences have been very briefly described in our previous work, but in a different context of 'parallel' supersequences:[25] here we go into substantially more depth about the development, and the relative merits of, the three different HSQC-COSY forms.

2 HSQC-CLIP-COSY

The first implementation is the direct usage of the HSQC-CLIP-COSY sequence as a NOAH module (Figure 2). In this sequence, a standard HSQC experiment is supplemented with a clean in-phase (CLIP) coherence transfer block, formed from a perfect echo[27–29] and a zero-quantum filter[26] (Figure 2). The spin echo of duration 4Δ just prior to detection allows for evolution of $^1J_{CH}$, meaning that the 'direct' responses acquire a negative sign, as illustrated in Figure 1c. Because of this inversion of direct responses, additional multiplicity editing in the HSQC step would lead to confusing spectra: thus, although the pulse sequences available on GENESIS do allow for multiplicity editing via an optional flag, they are omitted in the discussion which follows.
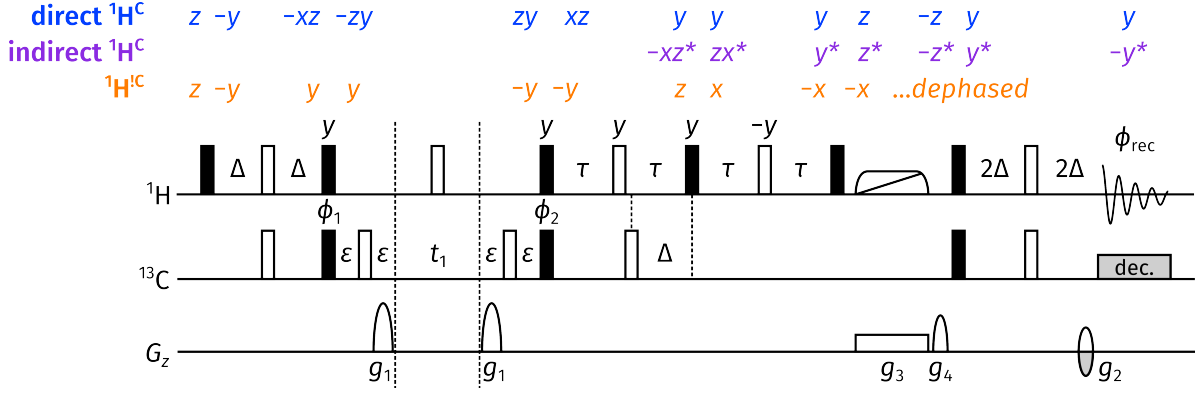
3

Figure 2: HSQC-CLIP-COSY experiment with product operator analysis for a three-spin *ISR* system, where I is ^{13}C, S is a directly bonded ^{1}H, and R a remote proton. Spins I and S are connected via one-bond ^{13}C–^{1}H scalar coupling, and S and R via a (typically three-bond) ^{1}H–^{1}H scalar coupling. Product operator analysis is provided for three relevant magnetisation pools: the 'direct ^{1}H^{C}' HSQC-type peaks, the 'indirect ^{1}H^{C}' responses which arise from coherence transfer from S to R in the perfect echo block, and the '^{1}H$^{!C}$' bulk magnetisation which we seek to preserve. Single-letter terms are shorthand for magnetisation on spin S (for example, x represents S_x); double-element terms to magnetisation on spins I and S (for example, xz is $2I_xS_z$). Letters with asterisks refer to magnetisation on the remote spin R; thus, for example, y^* means R_y, and xz^* means $2I_xR_z$. Solid bars are 90° pulses and empty bars 180° pulses; the rounded trapezoid and line represent an adiabatic inversion pulse. All pulses are applied along the $+x$-axis unless otherwise specified; the symbolic pulse phases are $\phi_1 = (x, -x)$; $\phi_2 = (x, x, -x, -x)$; and $\phi_{\text{rec}} = (x, -x, -x, x)$. Pulsed field gradient amplitudes are $g_1 = 37.10\,\text{G cm}^{-1}$ and $g_2 = 18.66\,\text{G cm}^{-1}$. The gradient g_3 should be calibrated as per Thrippleton et al.;[26] g_4 is a purge gradient with arbitrary amplitude. The delays Δ and τ are chosen to be $1/(4 \cdot {^1J_{\text{CH}}})$ and $1/(4 \cdot \sum {^nJ_{\text{HH}}})$; typically, $^1J_{\text{CH}}$ and $\sum {^nJ_{\text{HH}}}$ are respectively set as 145 Hz and 30 Hz, leading to values of $\Delta = 1.72$ ms and $\tau = 8.33$ ms. ε is the minimum time required for a pulsed field gradient plus a gradient recovery delay.

The main benefit of the HSQC-CLIP-COSY sequence is the pure absorption-mode lineshapes yielded by the CLIP transfer (Figure 3a). In this regard, it is the clear winner of all the sequences explored in this paper, as all the others generate a mixture of in-phase absorption and antiphase dispersion lineshapes. However, this comes at a price: there is no way for this sequence to preserve any magnetisation for later modules, as the product operator analysis shows: all unused magnetisation is dephased by the end of the sequence.

It is reasonable to question whether minor adjustments can be made to the pulse sequence to render it NOAH-compatible, as has previously been done for modules such as HMBC[21,30] and sensitivity-enhanced HSQC.[16,31] However, unfortunately, the CLIP element is wholly incompatible with preservation of unused magnetisation. Specifically, the zero-quantum filter dephases any magnetisation that is not along $\pm z$ at this time. However, if the 'bulk' ^{1}H$^{!C}$ magnetisation were to be placed along $\pm z$, there would be no way to later differentiate it from the 'indirect ^{1}H^{C}' magnetisation, since neither of these evolve under $^1J_{\text{CH}}$. Similar considerations preclude the possibility of variable ^{1}H^{C} excitation: if we had a portion of unused ^{1}H^{C} magnetisation
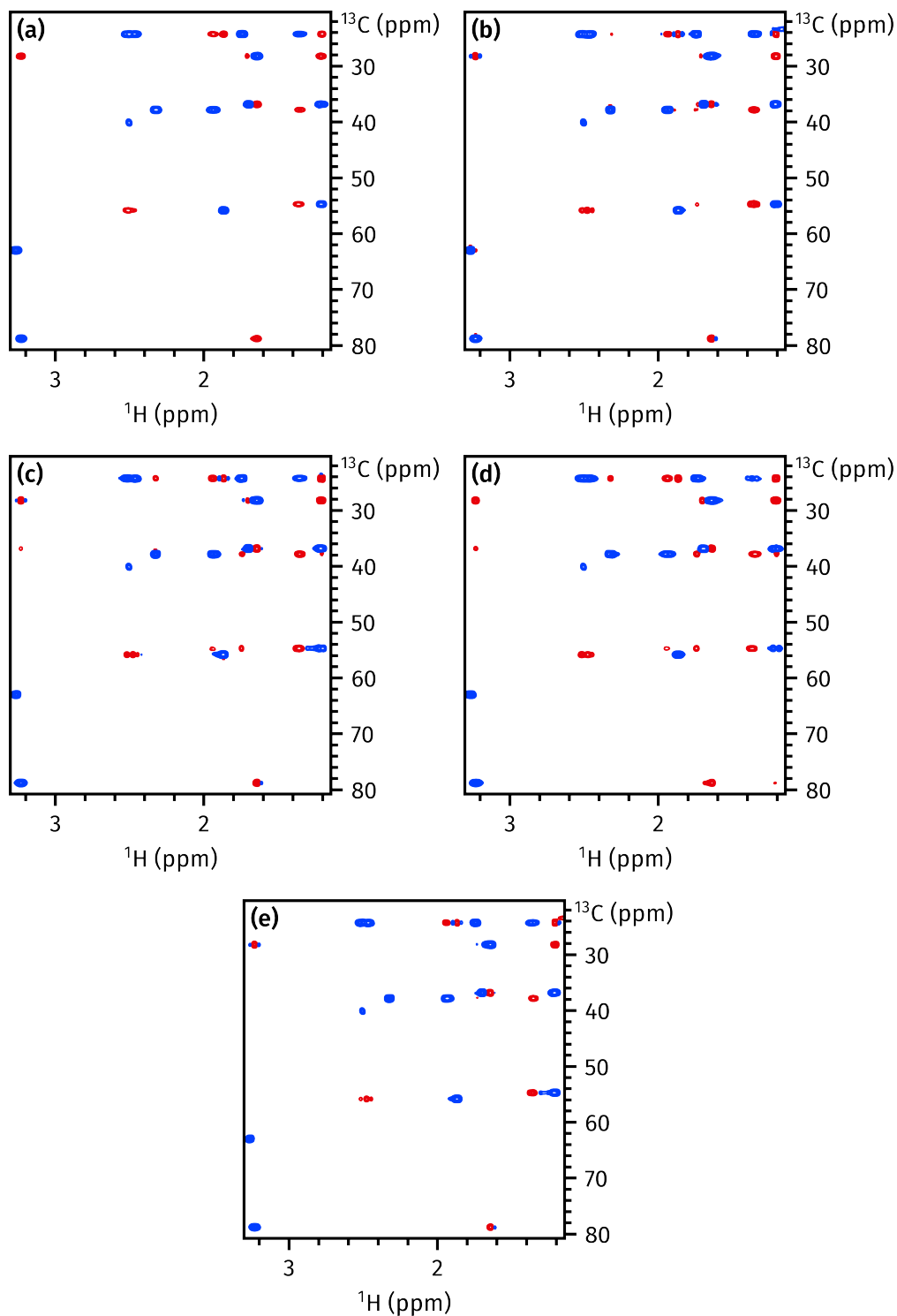
Figure 3: HSQC-COSY and HSQC-TOCSY spectra, taken from (respectively) NOAH-3 $S^C SC^c$ and NOAH-3 $S^T SC^c$ experiments. **(a)** HSQC-CLIP-COSY. **(b)** DSE HSQC-COSY. **(c)** TSE HSQC-COSY without suppression of relay artefacts (described in the text). **(d)** HSQC-TOCSY with 10 ms mixing time. **(e)** TSE HSQC-COSY with suppression of relay artefacts. Spectra were obtained on a 700 MHz Bruker AV III equipped with a TCI H/C/N cryoprobe; the sample used was 40 mM andrographolide in DMSO-d_6.
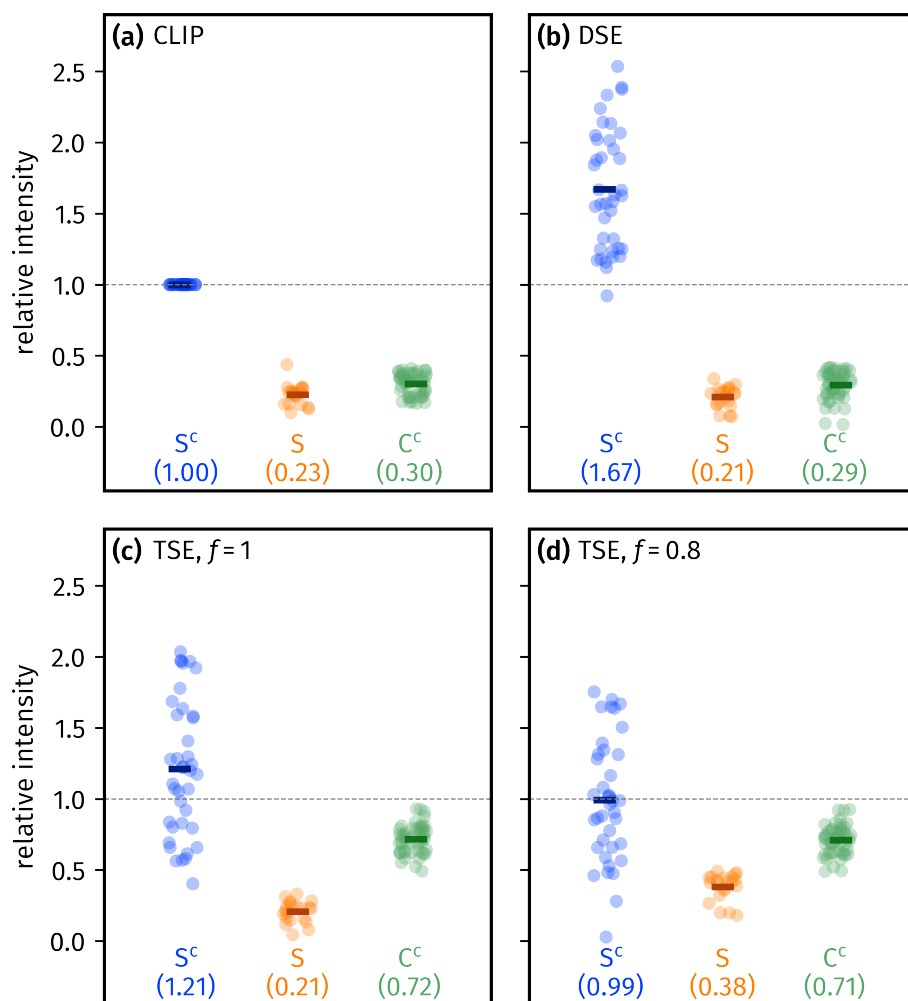
Figure 4: (Insert schematic of NOAH supersequence.) Sensitivity comparisons for all three modules in NOAH-3 $S^C SC^c$ (HSQC-COSY + HSQC + CLIP-COSY) supersequences, using a variety of implementations for the HSQC-COSY module. Peak intensities of the first module are measured relative to the HSQC-CLIP-COSY module itself (the leftmost column in (a)); whereas peak intensities of the HSQC and CLIP-COSY modules are measured relative to a separate, reference, NOAH-2 SC^c experiment. Numbers in parentheses indicate averages over all peaks. **(a)** HSQC-CLIP-COSY. **(b)** DSE HSQC-COSY. **(c)** TSE HSQC-COSY, acquired with $f = 1$. **(d)** TSE HSQC-COSY, acquired with $f = 0.8$. Spectra were obtained on a 700 MHz Bruker AV III equipped with a TCI H/C/N cryoprobe; the sample used was 40 mM andrographolide in DMSO-d_6.

that was intended to be stored for a subsequent module, this would have to be placed along the z-axis during the zero-quantum filter, but it cannot then be disentangled from the 'direct $^1H^{C}$' component which we do intend to detect.

A typical example of a NOAH supersequence featuring the HSQC-COSY module is a NOAH-3 $S^C SC^c$ supersequence (FIG 4A; S^C = HSQC-COSY, S = HSQC, and C^c = CLIP-COSY). From a practical perspective, the HSQC module can be configured to include, for example, multiplicity editing or coupling in F_2, which provides additional information not present in the HSQC-COSY. The CLIP-COSY module used here is simply a representative example of a homonuclear 2D

spectrum which frequently terminates a NOAH supersequence: it can be replaced with (amongst others) NOESY, ROESY, TOCSY, or even a PSYCHE pure shift spectrum.[15]

In the present work, however, this supersequence is chosen to illustrate the effect of varying the HSQC-COSY implementation on downstream modules. Because the HSQC-CLIP-COSY consumes all $^1H^C$ and $^1H^{!C}$ magnetisation, both the HSQC and CLIP-COSY which come after it only sample magnetisation that has recovered during the acquisition periods interspersed between modules. Thus, both of these modules have substantially reduced sensitivity (Figure 4a) when compared against a NOAH-2 SC^c supersequence (i.e., the same supersequence but with the HSQC-COSY removed).

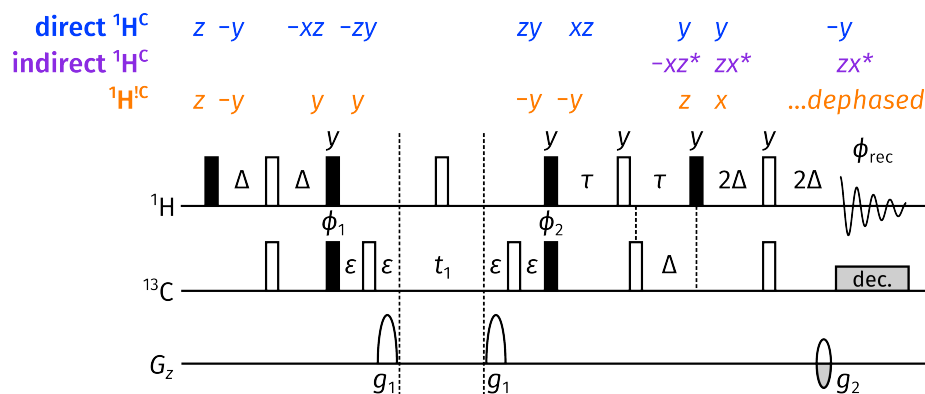# 3   Double spin echo HSQC-COSY

Figure 5: 'Double spin echo' HSQC-COSY experiment; all symbols have the same meaning as in Figure 2.

The purpose of the CLIP element in the HSQC-CLIP-COSY is to effect coherence transfer from one proton to another proton coupled to it. However, given that this CLIP element makes it impossible to preserve unused magnetisation, it is worth considering what happens when this is replaced with the simplest pulse sequence element for coherence transfer—namely, a spin echo followed by a 90° pulse. This simplification results in the 'double spin echo' (DSE) HSQC-COSY, so-named because it has two spin echoes after the t_1 period (Figure 5).

The removal of the CLIP element leads to mixed lineshapes in this experiment, where the direct responses are (mostly) in-phase absorption, and the indirect responses (mostly) antiphase dispersion. This is clearly visible in the spectrum (Figure 3b): the antiphase dispersion components are visible as 'wings' of opposite sign which flank each peak. On the other hand, because the antiphase magnetisation generated during the spin echo is not purged, the DSE HSQC-COSY sequence provides the greatest sensitivity of all the HSQC-COSY implementations here: for the sample used here, it yielded (on average) a 60% increase in sensitivity compared to the HSQC-CLIP-COSY. Unfortunately, as before, the DSE experiment does not preserve bulk magnetisation; it is

also incompatible with partial $^1\mathrm{H}^C$ excitation. Thus, the sensitivities of the subsequent modules in the NOAH-3 $\mathrm{S^C SC^c}$ supersequence remain very low (Figure 4b), and (accounting for noise) are identical to those seen previously with the HSQC-CLIP-COSY.
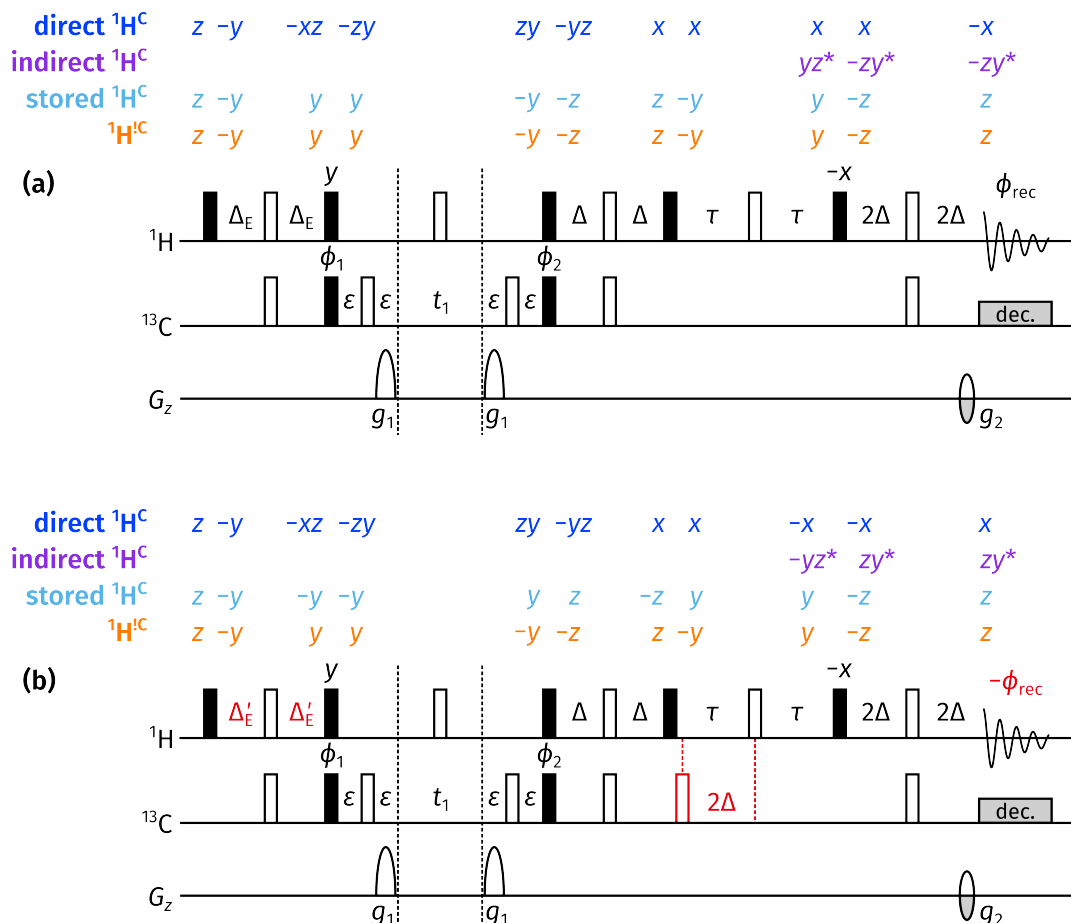
4 Triple spin echo HSQC-COSY

Figure 6: 'Triple spin echo' (TSE) HSQC-COSY experiment. **(a)** The first part of the experiment; this can be used on its own, but leads to spurious 'relayed' peaks arising via coherence transfer over two scalar couplings. **(b)** The second part of the experiment; co-adding this dataset with the first part leads to suppression of the relayed peaks. All symbols have the same meaning as in Figure 2.

We have seen that neither of the two HSQC-COSY implementations above (CLIP or DSE) could successfully preserve unused magnetisation. The triple spin echo (TSE) HSQC-COSY, shown in Figure 6, was developed as an alternative HSQC-COSY sequence which could. In terms of the pulse sequence itself,

OLD STUFF BELOW

In the DSE HSQC-COSY, the first of the two spin echoes after t_1 serves a dual purpose: $^1J_{CH}$ is allowed to evolve for a duration of $\tau - (\tau - \Delta) + \Delta = 2\Delta$ (thus generating peaks which are in-phase with respect to $^1J_{CH}$), and $^nJ_{HH}$ evolves for the total duration of 2τ (allowing coherence transfer to remote spins). The triple spin echo (TSE) HSQC-COSY is derived from the DSE version by separating the first spin echo into two distinct parts: one for $^1J_{CH}$ refocusing, and one for $^nJ_{HH}$ evolution. As shown by the product operator analysis in Figure 6a, this not only preserves the bulk $^1H^{1C}$ magnetisation, but is also compatible with partial $^1H^C$ excitation.

The problem with the TSE version is the spectral quality: consider an even larger spin system of the form $S-I-K-L$, where $\{I, K, L\}$ are ^1H and S is ^{13}C. At the end of t_1, single-quantum magnetisation on spin I is present. Any evolution of J_{IK} in the first spin echo (of duration 2Δ) leads to terms of the form $2I_yK_z$, and can then be transferred onto spin K by the subsequent 90°_x pulse. This magnetisation can then further evolve under J_{KL} during the 2τ spin echo, and then be transferred a *second* time by the 90°_{-x} pulse to spin L. Since the intensity of this transfer pathway is proportional to $\sin(2\pi J_{IK}\Delta)$, these 'relay' artefacts are especially prominent for large J_{IK}.

In order to suppress these, the experiment must be run a second time but with an additional 180° ^{13}C pulse inserted during the second spin echo (Figure 6b).[*] Any magnetisation still on spin I will therefore evolve under $^1J_{CH}$ for a total period of 4Δ, leading to net inversion. However, magnetisation which has already been transferred to spin K at this point will not be inverted: it is this magnetisation which is responsible for the relay artefacts. Therefore, by subtracting the two datasets (or equivalently, inverting the receiver phase and adding the two datasets), the desired peaks will be added up and the artefacts cancelled through subtraction.

The insertion of this 180° pulse also causes any unexcited $^1H^C$ magnetisation to be inverted. In order to ensure that this is returned to $+z$ at the end of the sequence (and not $-z$), the initial INEPT delay must be *lengthened* instead of shortened, as per:

$$\Delta'_E = \frac{2\Delta(\pi - \arcsin f)}{\pi},\tag{1}$$

where, as before, f is the proportion of magnetisation to be excited.

---

[*] A very similar strategy is used in the Bruker seHSQC pulse sequence `hsqcedetgpsisp2.4` to suppress the COSY-type artefacts. However, to the best of my knowledge, this sequence has not been published anywhere.

5 Supersequences

The spectral quality, and sensitivity, of all of these modules is captured in Figures 3 and 4. The CLIP version (Figures 3a and 4a) has the best lineshapes, but its sensitivity is slightly lower. The DSE version (Figures 3b and 4b) provides greater sensitivity, but at the cost of impure lineshapes.

For the TSE version, we first look at the importance of the relay artefact suppression procedure described above. The extra relay artefacts are clearly visible in Figure 3c, acquired using the 'basic' sequence in Figure 6a only. (As previously mentioned, these arise from large $^nJ_{HH}$ which evolve during the 2Δ spin echo; for this specific compound, the offending couplings are ^3J between two axial protons in a six-membered ring, and ^2J in diastereotopic methylenes). The presence of these peaks largely defeats the purpose of using an HSQC-COSY experiment; in fact, this unoptimised TSE HSQC-COSY is qualitatively very similar to an HSQC-TOCSY acquired with a short mixing time of 10 ms (Figure 3d).[†] However, these artefacts can be efficiently removed using the suppression technique described in the text above; the result in Figure 3e is qualitatively similar to the two other HSQC-COSY experiments. Using this suppression technique, the sensitivity of the TSE HSQC-COSY (when acquired with $f = 1$) falls between that of the CLIP and DSE versions.

Figure 4 also shows the relative sensitivities of the later modules in NOAH-3 $S^C SC^c$ superse-quences. In all of the first three cases (CLIP, DSE, and TSE HSQC-COSY with $f = 1$, Figures 4a to 4c), the HSQC sensitivity is low (ca. 20%) because no $^1H^C$ magnetisation is retained for it to use. Thus, the signal derives only from $^1H^C$ magnetisation which has recovered during the HSQC-COSY FID. However, when the TSE version is used, partial $^1H^C$ excitation can be used to control this sensitivity: for example, when $f = 0.8$ (Figure 4d), the HSQC-COSY sensitivity is decreased (on average equalling that of the HSQC-CLIP-COSY), but the sensitivity of the HSQC module is almost doubled. Generally, choosing a value of $f < 1$ allows for the HSQC-COSY and HSQC sensitivities to be better balanced.

Finally, the CLIP-COSY module suffers when the HSQC-CLIP-COSY or the DSE HSQC-COSY are used, because both of these dephase $^1H^{!C}$ magnetisation; however, the TSE version success-fully preserves around 70% of this magnetisation for it, regardless of the value of f. (This value is slightly lower than the approximately 90% magnetisation preserved by the HSQC module, be-cause the bulk magnetisation is placed in the transverse plane during the 2τ spin echo (Figure 6a) and experiences losses due to $^nJ_{HH}$ evolution.)

[†]The HSQC-TOCSY even gives better peak shapes, since the DIPSI mixing transfers in-phase magnetisation to in-phase magnetisation.
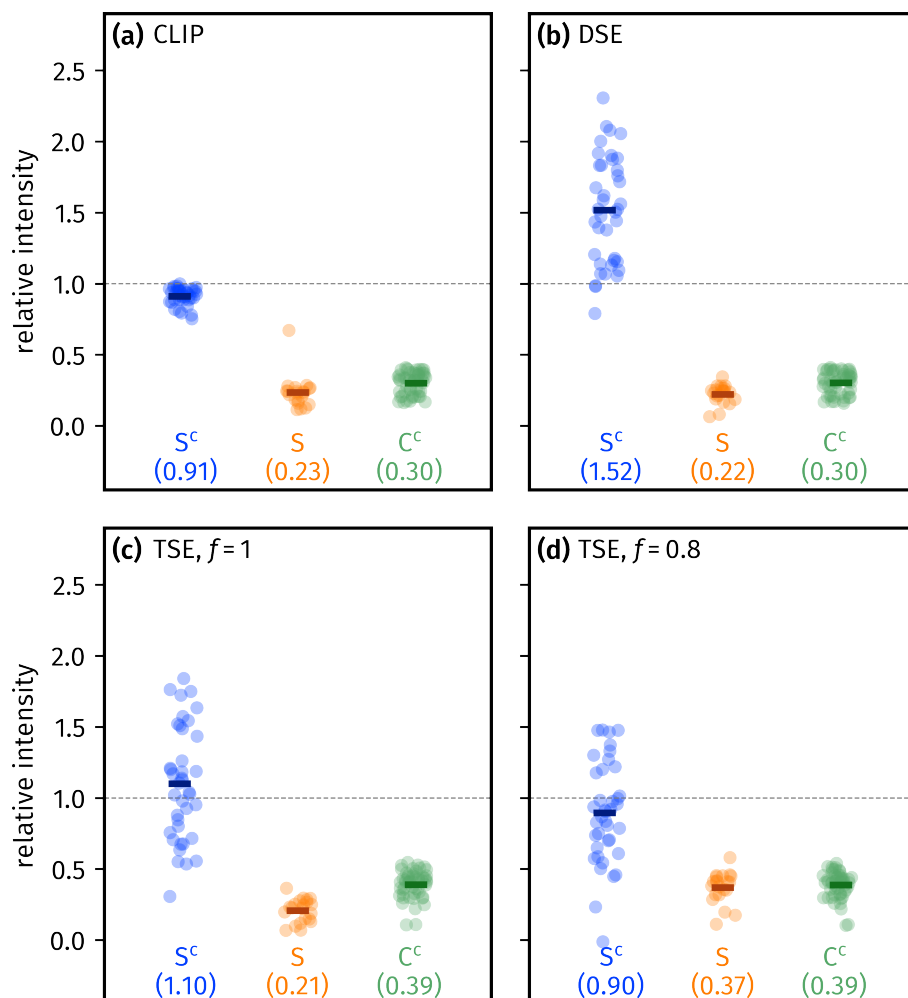
6 HSQC-COSY in context

Figure 7: Sensitivity comparisons for the three last modules in NOAH-4 BS^CSC^c supersequences. Peak intensities are relative to the HSQC-CLIP-COSY module from a NOAH-3 S^CSC^c supersequence, and HSQC and CLIP-COSY spectra from a NOAH-2 SC^c experiment (these are the same reference spectra as used in Figure 4). Numbers in parentheses indicate averages over all peaks. **(a)** HSQC-CLIP-COSY. **(b)** DSE HSQC-COSY. **(c)** TSE HSQC-COSY, acquired with $f = 1$. **(d)** TSE HSQC-COSY, acquired with $f = 0.8$. 7A-210723

In NOAH-3 S^CSC^c-type supersequences, using the TSE HSQC-COSY module here appears to be a sensible option as it is capable of preserving some $^1H^C$ magnetisation for the HSQC, as well as all $^1H^{IC}$ magnetisation for the CLIP-COSY. However, this may not necessarily be so important in the context of a larger supersequence—particularly one which begins with the HMBC module, which *already* dephases $^1H^{IC}$ magnetisation (meaning that there is not much of it to preserve).

Figure 7 provides the same sensitivity comparisons as in Figure 4, but in the context of a NOAH-4 BS^CSC^c supersequence instead. The HSQC-COSY and HSQC modules largely follow the same pattern as before, but with an approximate 10% loss across the board: this reflects the imperfect preservation of $^1H^C$ magnetisation by the zz-HMBC module. The CLIP-COSY module, however,

has a substantially lower sensitivity regardless of which HSQC-COSY module is chosen. When the CLIP or DSE HSQC-COSY modules are used, the CLIP-COSY retains only roughly 30% of its original intensity: this is the same as in Figure 4. With the TSE HSQC-COSY, this is boosted to around 40% because there is one extra FID in which the $^1\mathrm{H}^{1\mathrm{C}}$ polarisation can be recovered. However, the use of the HMBC module at the beginning effectively places an upper limit on the amount of signal available to this module.

For virtually all homonuclear modules (including the CLIP-COSY), this small difference in sensitivity will not make a real difference in the interpretability of the spectrum. This is especially so considering that the HMBC module—which has a far lower sensitivity—is also present in the supersequence: a CLIP-COSY with 30% of its original sensitivity is still more intense than the HMBC experiment. This argument was used in justifying the NOAH-3 BSC^c experiment, and logically, should be equally applicable to the NOAH-4 BS^{C}SC^c experiment. In this case, the only compelling reason to use the TSE HSQC-COSY would be to preserve a portion of $^1\mathrm{H}^C$ magnetisation for a later ^{13}C module. Thus, in this context, the decision of which HSQC-COSY module to use is slightly more nuanced: the cleaner lineshapes provided by the CLIP version, or the sensitivity of the DSE version, may be more preferable.

Acknowledgements

References

(1) Frydman, L.; Scherf, T.; Lupulescu, A. The acquisition of multidimensional NMR spectra within a single scan. *Proc. Natl. Acad. Sci. U. S. A.* **2002**, *99*, 15858–15862, DOI: 10.1073/pnas.252644399.

(2) Pelupessy, P. Adiabatic Single Scan Two-Dimensional NMR Spectrocopy. *J. Am. Chem. Soc.* **2003**, *125*, 12345–12350, DOI: 10.1021/ja034958g.

(3) Frydman, L.; Lupulescu, A.; Scherf, T. Principles and Features of Single-Scan Two-Dimensional NMR Spectroscopy. *J. Am. Chem. Soc.* **2003**, *125*, 9204–9217, DOI: 10.1021/ja030055b.

(4) Kazimierczuk, K.; Stanek, J.; Zawadzka-Kazimierczuk, A.; Koźmiński, W. Random sampling in multidimensional NMR spectroscopy. *Prog. Nucl. Magn. Reson. Spectrosc.* **2010**, *57*, 420–434, DOI: 10.1016/j.pnmrs.2010.07.002.

(5)   Mobli, M.; Hoch, J. C. Nonuniform sampling and non-Fourier signal processing methods in multidimensional NMR. *Prog. Nucl. Magn. Reson. Spectrosc.* **2014**, *83*, 21–41, DOI: `10.1016/j.pnmrs.2014.09.002`.

(6)   Kazimierczuk, K.; Orekhov, V. Non-uniform sampling: post-Fourier era of NMR data collection and processing. *Magn. Reson. Chem.* **2015**, *53*, 921–926, DOI: `10.1002/mrc.4284`.

(7)   Kupče, Ē.; Freeman, R.; John, B. K. Parallel Acquisition of Two-Dimensional NMR Spectra of Several Nuclear Species. *J. Am. Chem. Soc.* **2006**, *128*, 9606–9607, DOI: `10.1021/ja0634876`.

(8)   Kupče, Ē.; Freeman, R. Molecular Structure from a Single NMR Experiment. *J. Am. Chem. Soc.* **2008**, *130*, 10788–10792, DOI: `10.1021/ja8036492`.

(9)   Kovacs, H.; Kupče, Ē. Parallel NMR spectroscopy with simultaneous detection of ^{1}H and ^{19}F nuclei. *Magn. Reson. Chem.* **2016**, *54*, 544–560, DOI: `10.1002/mrc.4428`.

(10)   Kupče, Ē.; Freeman, R. Fast multidimensional NMR by polarization sharing. *Magn. Reson. Chem.* **2007**, *45*, 2–4, DOI: `10.1002/mrc.1931`.

(11)   Schulze-Sünninghausen, D.; Becker, J.; Luy, B. Rapid Heteronuclear Single Quantum Correlation NMR Spectra at Natural Abundance. *J. Am. Chem. Soc.* **2014**, *136*, 1242–1245, DOI: `10.1021/ja411588d`.

(12)   Becker, J.; Koos, M. R. M.; Schulze-Sünninghausen, D.; Luy, B. ASAP-HSQC-TOCSY for fast spin system identification and extraction of long-range couplings. *J. Magn. Reson.* **2019**, *300*, 76–83, DOI: `10.1016/j.jmr.2018.12.021`.

(13)   Kupče, Ē.; Claridge, T. D. W. NOAH: NMR Supersequences for Small Molecule Analysis and Structure Elucidation. *Angew. Chem. Int. Ed.* **2017**, *56*, 11779–11783, DOI: `10.1002/anie.201705506`.

(14)   Yong, J. R. J.; Kupče, Ē.; Claridge, T. D. W. In *Fast 2D solution-state NMR: concepts and applications*, Giraudeau, P., Dumez, J.-N., Eds.; Royal Society of Chemistry: London, UK, 2023, DOI: `10.1039/BK9781839168062-00084`.

(15)   Yong, J. R. J.; Kupče, Ē.; Claridge, T. D. W. Modular Pulse Program Generation for NMR Supersequences. *Anal. Chem.* **2022**, *94*, 2271–2278, DOI: `10.1021/acs.analchem.1c04964`.

(16)   Yong, J. R. J.; Hansen, A. L.; Kupče, Ē.; Claridge, T. D. W. Increasing sensitivity and versatility in NMR supersequences with new HSQC-based modules. *J. Magn. Reson.* **2021**, *329*, 107027, DOI: `10.1016/j.jmr.2021.107027`.

(17)   Nyberg, N. T.; Duus, J. Ø.; Sørensen, O. W. Heteronuclear Two-Bond Correlation: Suppressing Heteronuclear Three-Bond or Higher NMR Correlations while Enhancing Two-Bond Correlations Even for Vanishing $^2J_{CH}$. *J. Am. Chem. Soc.* **2005**, *127*, 6154–6155, DOI: `10.1021/ja050878w`.

(18)   Nyberg, N. T.; Duus, J. Ø.; Sørensen, O. W. Editing of H2BC NMR spectra. *Magn. Reson. Chem.* **2005**, *43*, 971–974, DOI: `10.1002/mrc.1698`.

(19)   Kupče, Ē.; Sørensen, O. W. 2BOB - extracting an H2BC and an HSQC-type spectrum from the same data set, and H2OBC - a fast experiment delineating the protonated ^{13}C backbone. *Magn. Reson. Chem.* **2017**, *55*, 515–518, DOI: `10.1002/mrc.4584`.

(20) Hu, K.; Westler, W. M.; Markley, J. L. Two-dimensional concurrent HMQC-COSY as an approach for small molecule chemical shift assignment and compound identification. *J. Biomol. NMR* **2011**, *49*, 291–296, DOI: `10.1007/s10858-011-9494-4`.

(21) Kupče, Ē.; Claridge, T. D. W. New NOAH modules for structure elucidation at natural isotopic abundance. *J. Magn. Reson.* **2019**, *307*, 106568, DOI: `10.1016/j.jmr.2019.106568`.

(22) Gyöngyösi, T.; Timári, I.; Haller, J.; Koos, M. R. M.; Luy, B.; Kövér, K. E. Boosting the NMR Assignment of Carbohydrates with Clean In-Phase Correlation Experiments. *ChemPlusChem* **2018**, *83*, 53–60, DOI: `10.1002/cplu.201700452`.

(23) Gyöngyösi, T.; Timári, I.; Sinnaeve, D.; Luy, B.; Kövér, K. E. Expedited Nuclear Magnetic Resonance Assignment of Small- to Medium-Sized Molecules with Improved HSQC-CLIP-COSY Experiments. *Anal. Chem.* **2021**, *93*, 3096–3102, DOI: `10.1021/acs.analchem.0c04124`.

(24) Orts, J.; Gossert, A. D. Structure determination of protein-ligand complexes by NMR in solution. *Methods* **2018**, *138-139*, 3–25, DOI: `10.1016/j.ymeth.2018.01.019`.

(25) Kupče, Ē.; Yong, J. R. J.; Widmalm, G.; Claridge, T. D. W. Parallel NMR Supersequences: Ten Spectra in a Single Measurement. *JACS Au* **2021**, *1*, 1892–1897, DOI: `10.1021/jacsau.1c00423`.

(26) Thrippleton, M. J.; Keeler, J. Elimination of Zero-Quantum Interference in Two-Dimensional NMR Spectra. *Angew. Chem., Int. Ed.* **2003**, *42*, 3938–3941, DOI: `10.1002/anie.200351947`.

(27) Aguilar, J. A.; Nilsson, M.; Bodenhausen, G.; Morris, G. A. Spin echo NMR spectra without J modulation. *Chem. Commun.* **2012**, *48*, 811–813, DOI: `10.1039/c1cc16699a`.

(28) Parella, T. Towards perfect NMR: Spin-echo versus perfect-echo building blocks. *Magn. Reson. Chem.* **2019**, *57*, 13–29, DOI: `10.1002/mrc.4776`.

(29) Koos, M. R. M.; Kummerlöwe, G.; Kaltschnee, L.; Thiele, C. M.; Luy, B. CLIP-COSY: A Clean In-Phase Experiment for the Rapid Acquisition of COSY-type Correlations. *Angew. Chem., Int. Ed.* **2016**, *55*, 7655–7659, DOI: `10.1002/anie.201510938`.

(30) Claridge, T. D. W.; Mayzel, M.; Kupče, Ē. Triplet NOAH supersequences optimised for small molecule structure characterisation. *Magn. Reson. Chem.* **2019**, *57*, 946–952, DOI: `10.1002/mrc.4887`.

(31) Hansen, A. L.; Kupče, Ē.; Li, D.-W.; Bruschweiler-Li, L.; Wang, C.; Brüschweiler, R. 2D NMR-Based Metabolomics with HSQC/TOCSY NOAH Supersequences. *Anal. Chem.* **2021**, *93*, 6112–6119, DOI: `10.1021/acs.analchem.0c05205`.

Supporting Information

for

Title?

Jonathan R. J. Yong,[1] Ēriks Kupče,[2] Tim D. W. Claridge[1,*]

[1] *Chemistry Research Laboratory, Department of Chemistry, University of Oxford, Mansfield Road, Oxford OX1 3TA, United Kingdom*

[2] *Bruker UK Ltd, R&D, Coventry CV4 9GH, United Kingdom*

[*] `tim.claridge@chem.ox.ac.uk`

Contents

S1 Software and raw data

All processing was carried out using TopSpin 3 or 4. Plots are generated in Python 3, using the `numpy`, `scipy`, and `penguins` libraries. The raw data used for this paper, as well as all scripts required for regenerating the plots, are available on GitHub: `https://github.com/yongrenjie/hsqc-cosy-paper`.